Computer Fraud and Security
ISSN (online): 1873-7056

Deep Learning-Based Approach for Early Detection of Osteoporosis Using X-ray Imaging

B P Pradeep Kumar[1], G.R.Poornima[2], Sanjay H S[3], Anil Kumar C[4], Lavanya Vaishnavi D A[5]

[1]Professor, Dept. of Computer Science & Design, Atria Institute of Technology, Bengaluru, India, pradi14cta@gmail.com

[2]Department of Electronics and Communication engineering, Sri Venkateshwara College of Engineering, Bangalore, India, poornima_g_r@yahoo.com

[3]Manager - Data Solutions & Insights, Vision Care, Carl Zeiss India, Pvt Ltd, Bangalore, sanjaymurthyhs@gmail.com

[4]Professor & HoD, Dept of ECE, R L Jalappa Institute of Technology, Doddaballapur, India, canilkumarc22@gmail.com

[5]Assistant Professor, Dept of ECE, R L Jalappa Institute of Technology, Doddaballapur, India

lavanyavaishnavi@gmail.com

Abstract ---

The main cause of factures in women and older adults after menopause is osteoporosis, a disorder that weakens bones. The start of an inexpensive technology for simpler detection is required because of the current expense of diagnosis and treatment procedures. Although X-ray imaging is widely available and reasonably priced, it has drawbacks in terms of computationally demanding feature extraction and manual interpretation. A CNN-based method that used transfer learning was used to categorise knee X-ray pictures into three groups: normal, osteopenia, and osteoporosis. A dataset of 381 knee radiographs to T-score from Quantitative Ultrasound, which has been medically validated, was used to assess four pre-trained CNN architectures: AlexNet, VGG16, ResNet, and VGG-19. The AlexNet model outperformed non-pretrained models by a vast margin, attaining 91.1% accuracy, anerror ratio of 0.09, and a validation loss of 0.54.

Index Terms—Osteoporosis, Deep Learning, Transfer Learning, X-ray Imaging, AlexNet, Medical Imaging.

I. Introduction

The most widely used imaging method in the medical field for identifying bone diseases is X-ray imaging. The oldest and most widely used method for taking pictures of practically every bone in the body, including the wrist, knee, elbow, shoulder, knee, pelvis, spine, etc., is X-ray. X-ray imaging aids in the identification of fractures, joint dislocations, bone damage, aberrant bone growth, infections, and even arthritis. Although they are mostly unintentional, bone fractures can also be pathological. This is because osteoporosis, cancer, or osteogenesis can weaken bones.The primary bone disease that causes millions of fractures globally is osteoporosis , with a higher prevalence among women. Although osteoporosis is associated with aging because bones weaken with age, it can also occur at younger ages. Because its symptoms are not apparent in the early stages and become more

noticeable when osteoporosis has progressed to a point where bones are vulnerable to fractures with a slight fall, osteoporosis is also known as the silent illness. Economic resources are heavily depleted by the expenditures of osteoporosis treatment, including fracture repair. Therefore, early diagnosis is necessary to lower treatment

costs[18,19].

Using the Dual Energy X-ray Absorptiometry Technique (DXA), osteoporosis is medically diagnosed. It calculates the bone mineral density (BMD) for various stages of osteoporosis using the T-score and Z-score values that have been approved by the WHO[20,21]. However, there are certain drawbacks, such as the technique's high cost and limited availability for areal measurements. The Quantitative Ultrasound System (QUS), Computed Tomography (CT), and Magnetic Resonance Imaging (MRI) are further imaging modalities used to identify osteoporosis. MRI is a 3 T enhanced bone microarchitecture imaging technology, but it is highly expensive and has a reduced spatial resolution [22].

Deep learning-based convolutional neural network (CNN) techniques have become more and more popular among CAD systems for medical image analysis in recent years because of their cutting-edge outcomes in identifying a variety of diseases from images, including multiple sclerosis, brain tumors, breast cancer, pneumonia, and cancer detection as well as human activity recognition. In the classification of medical pictures, CNNs such as AlexNet, ResNet-50, VGG-16, VGG-19, and GoogleNet have demonstrated cutting-edge performance. The biggest problem with CNN classifiers is that they require a large amount of labeled data for training, yet it can be quite challenging to find large datasets in the medical area. Researchers have developed the concept of transfer learning to address this problem.

In this study, we have developed an early detection system for osteoporosis in the knee by utilizing the strength of CNN topologies and the affordability of X-ray imaging. Our model classifies the knee X-ray images using deep learning algorithms and the well- known CNNs AlexNet, VggNet-16, ResNet, and VggNet-19.

II. Literature Review

Deep learning has revolutionized the field of medical imaging, and significant advancement in disease detection have been seen. For osteoporosis detection, the deep learning approaches have emerged from traditional cascaded pipelines to more advanced end models.

A. Traditionally, osteoporosis diagnosis is done using technique like Dual-Energy X-ray Absorptiometry (DXA) and manual X-ray image interpretation. Whereas DXA is the gold standard to estimate the bone density, it involves expense and time, which poses a limitation to its usage. Manual interpretation is, however, prone to inter-radiologist variability.[23][24]

B. Deep Learning Models for Automated Detection With the end- to-end deep learning models, osteoporosis detection has been transformed from a manually feature-extracting task to a much more accurate process. Specifically, CNNs have proven very successful in pattern recognition directly in X-ray images of bone structures. ResNet, VGG, and DenseNet architectures were fine- tuned on large datasets for medical image tasks, which learn the complex representations.[25].

C. Transfer learning and domain adaptation are two of the most successful techniques in dealing with the sparse data issue for osteoporosis detection. Fine-tuning a pre-trained model on medical X-ray datasets, which are already trained on ImageNet, can be an affordable approach in low-resource settings. Recently, public 3 databases such as MURA and OAI are being developed to help overcome the data scarcity issue.[26][27].

D. Frameworks and Toolkits are Pre-trained models included in toolkits and frameworks such as PyTorch and TensorFlow enabled researchers to implement deep learning approaches rather efficiently. Several augmentation methods are supported in the platforms so that models for the detection of osteoporosis can easily be adapted. More specialized medical imaging tools like segmentation, classification, and others exist in frameworks like MONAI for Medical Open Network for AI.[28]

E. Practical Applications and Challenges Such as deep learning models can be applied in real-time to screen for osteoporosis and make early diagnoses. Heatmap visualizations help radiologists understand model predictions, thus making a connection between AI and clinical practice. Challenges remain, however, in generalizing to

various patient populations and maintaining interpretability in decision-making.[29]

Key Challenges and Future Directions:

Data Scarcity: Creating high-quality, annotated datasets remains a priority. Methods like data augmentation and weak supervision can help bridge the gap.[30]

Generalization Across Populations: There are emerging research directions in the context of domain adaptation and federated learning to boost performance on heterogeneous populations.[31]

Integrate with existing systems: Combination of AI-based solutions with traditional diagnostic methods, like DXA, will further improve the accuracy and confidence of diagnosis.[15]

Table 1: Comparative Analysis of Additional References in Detection of Osteoporosis

Citations	Reliability	Advantage	Disadvantage
[1]	High: Printed in a respectable engineering publication.	explains how to design the Kogge Stone Adder efficiently utilizing cutting-edge VLSI techniques	Lacks practical implementation ideas and is restricted to CMOS and GDI design.
[2]	High: A peer- reviewed journal	U-Net topologies provide improved glaucoma detection accuracy.	Limited generalizability due to its exclusive focus on U-Net and U-Net+ designs.
[3]	High: J Magn Reson Imaging published it.	thorough evaluation of machine learning techniques' performance in fracture prediction.	Restricted to fragility fractures and MRI data only.
[4]	High: Printed in a reputable publication for computation	Offers a thorough evaluation of machine learning methods for predicting glucose intolerance.	Does not explore other predictive factors beyond glucose intolerance risk.
[5]	Moderate: Printed in a national publication.	A new way for American Sign Language is provided by the hybrid gesture recognition technique.	has a small dataset and is not globally applicable.
[6]	High printed in a respectable publication of computational biology.	Efficient employing modern imaging to identify prostate cancer by utilizing histology	It might not be immediately applicable to other imaging modalities or cancer types.
[7]	High - Acsessable through SSRN	Prostate melanoma can be better assessed radiographically with the VBIR technique	Restricted to patientswith prostate melanoma it might not spread to other tumors
[8]	High: Printed in proceedings of the IEEE Conference.	creative application of bar opodometry to evaluate postmenopausal women's bone mineral density	Restricted to particular experimental settings and postmenopausal women.
[9]	Moderate: Printed in a publication with a broad focus on IoT.	presentsa revolutionary robotics-based Internet of Things solution for rubbish accumulation	lacks information regarding long- term maintenance and scalability.
[10]	High: A conference paper that is peer- reviewed.	Using CT scans, CNN-based automated detection provides an effective osteoporosis screening technique.	focuses mostly on CT scans, with scant attention to other imaging modalities.
[11]	Excellent: resented an IEEE conference	Simulation Based Detailed design and analysis of UHF BJT Feedback oscillators.	Restricted to Particular uses in communication systems and the UHF range.
[12]	High: J College Radiol published it.	Uses Deep learning to simulate dual-energy X-ray absorptiometry for	Limited to CT Data acess to high-quality imaging datasets

		accurate bone analysis	is necessary.
[13]	Moderate: Printed in the proceedings of the Springer conference.	Kinect sensor used effectively for gesture detection in American Sign Language	focuses on Kinect-based devices; other platforms are not given as much flexibility.
[14]	High: Eur Radiol published it	Bone susceptibility mapping using MRI provides a trustworthy biomarker for examines	Is expensive since it necessitates access to MRI facilities.
[15]	High: SN Computational Science published it	the efficacy of deep learning in processing hematological images	hematological samples; it has few medical applications.
[16]	J Smart Health published a high-quality article.	Using dental radiographs and sophisticated feature learning, multitask learning is used for osteoporosis pre screening	Restricted to radiography of the teeth, which could not include all risk variables.
[17]	High Accessible via SSRN.	Centered using ultrasonic images in an automated manner to diagonise liver cancer	It is Exclusive to identifying liver tumors and does not generalize to other type of cancers.

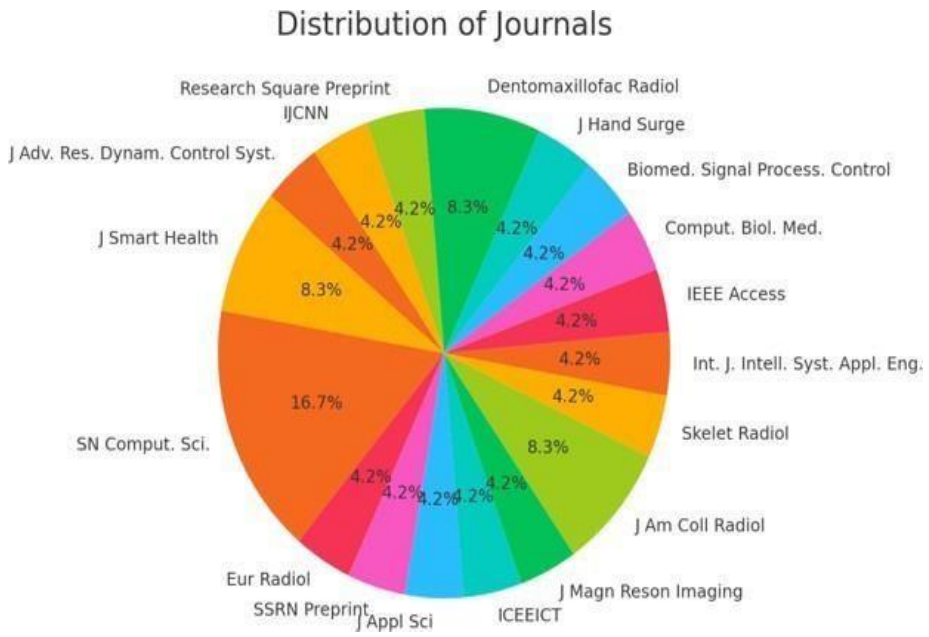

Figure 1. Distribution of Publications

Figure 1 Illustrates: The distribution of publications among various journals is depicted in this pie chart, where each slice represents a particular journal and its size indicates the percentage of articles published there. For example, the largest chunk (16.7%) is occupied by SN Comput. Sci., suggesting that it is the most often published journal in the dataset. Notable but smaller contributions are made by several journals, including IEEE Access, J Magn Reson Imaging, and Eur Radiol. A tiny number of journals, including SSRN Preprint, J Smart Health, and Dentomaxillofac Radiol, each account for 4.2% of the total. In conclusion, the figure provides a general picture of how publications are distributed throughout different journals.

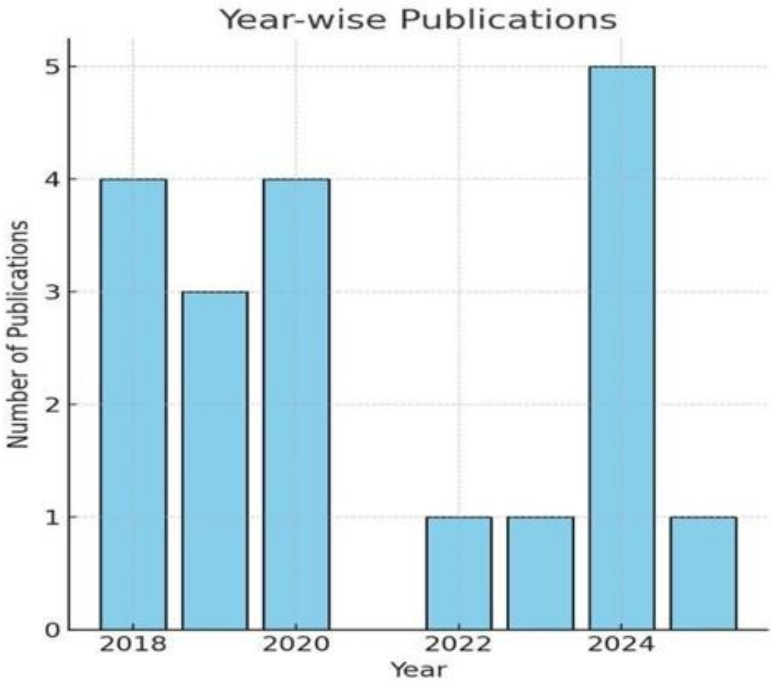

Figure 2. Year-wise Distribution of Publications

Figure 2 Illustrates the distribution of detection of osteoporosis research publication by year.In the past ten years, the graph shows a steady increment in research activities, The distribution of publications pertaining to (supposedly) osteoporosis detection studies over a number of years is depicted in the bar graph. The y- axis shows the quantity of publications, while the x-axis shows the year, which spans from 2018 to 2024. The graph shows that there was a range of scientific activities throughout this time.

Both 2018 and 2020 saw four publications, suggesting a steady level of interest during those years. With just three publications in 2019, there is a minor decline. With just one publication annually, 2022 and 2023 see a more notable decline. Nonetheless, 2024 shows a significant increase in research production, with five publications—the most throughout the period under observation.

III. METHODOLOGY

A. Overview of System

In this study, we evaluated four state-of-the-art pretrained convolutional neural network (CNN) architectures - AlexNet,VGG-16, VGG-19, and ResNet – due to their demonstrated success and widespread application in medical image classification tasks. These architectures have been extensively validated in previous studies for their ability to extract robust features from complex image datasets, making them ideal candidates for our task of. osteoporosis detection.

Transfer learning was used as the main strategy in this study in order to optimize the benefits of pre-trained models. Transfer learning makes it possible to fine-tune weights from models that have previously been trained on sizable datasets, like ImageNet, for the particular classification task at hand. By using this technique, the model may apply the information it has acquired from extensive training on a variety of data to the specific objective of classifying knee X-ray pictures for the detection of osteoporosis.

The architecture's last classification layers were one of the main changes undertaken. A new layer specifically designed for our objective was added to the pre-trained models' final completely connected layers. After adding a dense layer,

a softmax activation function was used to generate the probability of classifying the images as normal, osteoporotic, or non-osteoporotic.

To improve performance on our particular dataset, the weights of the pre-trained layers were adjusted rather than frozen. While maintaining the fundamental feature extraction skills acquired during the pretraining stage, this fine-tuning procedure entailed retraining some or all of the layers to adjust to the unique characteristics of our X-ray images. As a result, the model was better able to diagnose osteoporosis by capturing the subtleties of knee X-ray pictures.

Another important component of the model enhancement process was performance optimization. To improve convergence, a variety of hyperparameter optimization strategies were used to adjust parameters including learning rates, dropout rates, and activation functions. To identify the model that provided the best balance of precision, recall, and overall accuracy in identifying osteoporosis from knee X-rays, the designs were thoroughly assessed.

There were various benefits to using transfer learning in this situation. It drastically cut down on training time, to start. Compared to training from scratch, the models took significantly less time to converge when pre-trained weights were used. It also enhanced generalization. The model has a solid foundation thanks to the pre-trained weights, which were first trained on a sizable and varied dataset like ImageNet. This allowed the model to generalize more successfully on our comparatively smaller dataset. Last but not least, pre-trained layers performed exceptionally well in obtaining low-level and mid-level characteristics, like edges and textures, which are essential for differentiating between various bone states.

All things considered, evaluating the effectiveness of various architectures has given important information on which model is most suited for the task of identifying osteoporosis from knee X-ray pictures.

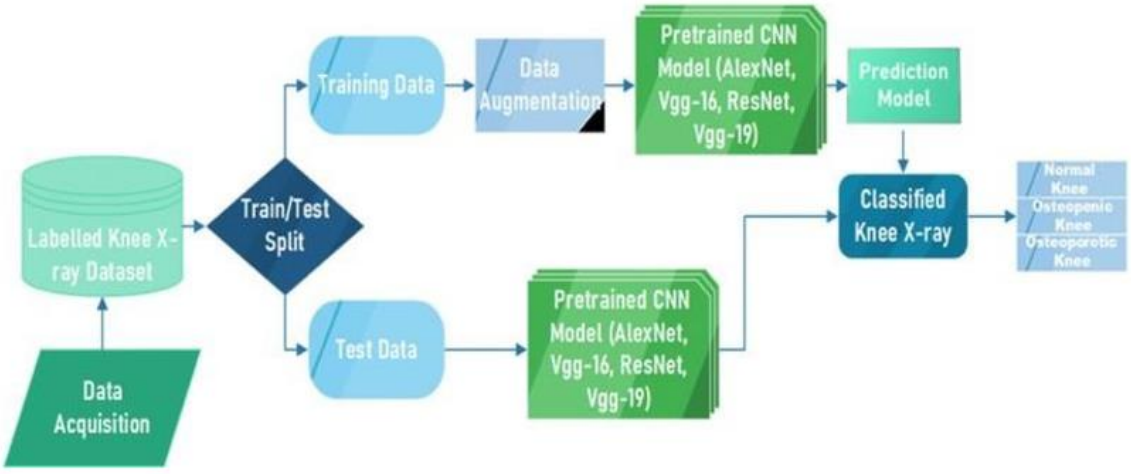

Figure 3. Data Pre-processing and Training Flowchart

Figure 3 Illustrates the method for detecting osteoporosis using pre-trained CNNs and knee X-ray pictures. Training and testing sets are created from a labeled X-ray dataset, with the training set receiving data augmentation. A prediction model uses the characteristics extracted from both sets by pre- trained models (AlexNet, VGG-16, ResNet, and VGG-19) to categorize X-rays into normal, osteopenic, and osteoporotic osteoporosis. This method effectively detects osteoporosis by using transfer learning.

A number of crucial measures and mathematical operations are frequently employed to assess model performance in the context of osteoporosis detection utilizing knee X-rays and deep learning models such as CNNs (Convolutional Neural Networks) and Transfer Learning. These metrics aid in evaluating the model's ability to detect, classify, and generalize to new data.

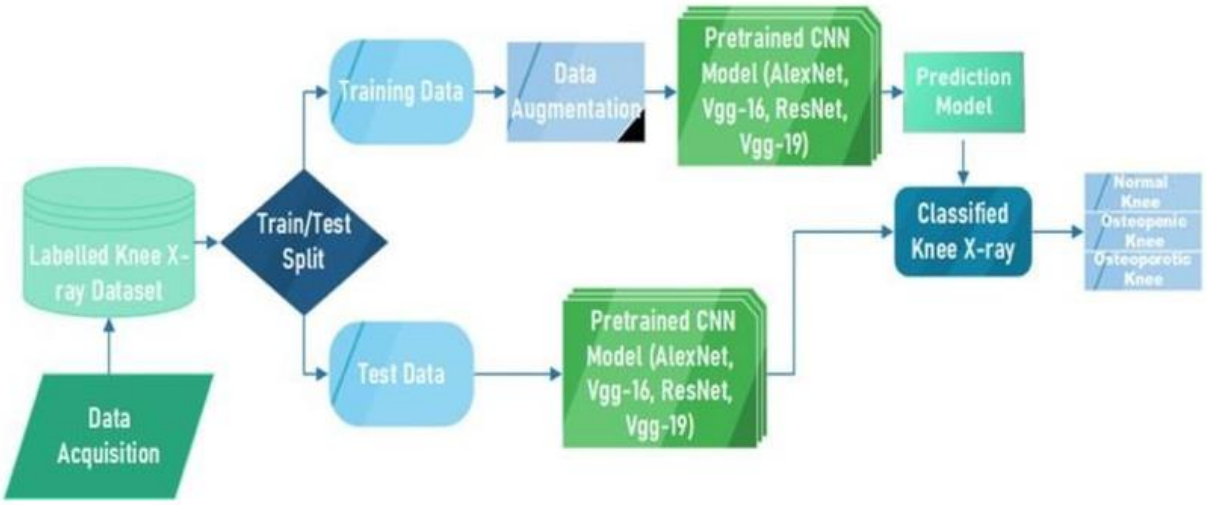

Figure 3. Data Pre-processing and Training Flowchart

Figure 3 Illustrates the method for detecting osteoporosis using pre-trained CNNs and knee X-ray pictures.

Training and testing sets are created from a labeled X-ray dataset, with the training set receiving data augmentation. A prediction model uses the characteristics extracted from both sets by pre- trained models (AlexNet, VGG-16, ResNet, and VGG-19) to categorize X-rays into normal, osteopenic, and osteoporotic osteoporosis. This method effectively detects osteoporosis by using transfer learning.

A number of crucial measures and mathematical operations are frequently employed to assess model performance in the context of osteoporosis detection utilizing knee X-rays and deep learning models such as CNNs (Convolutional Neural Networks) and Transfer Learning. These metrics aid in evaluating the model's ability to detect, classify, and generalize to new data.

B. Accuracy

The percentage of accurate predictions the model makes out of all forecasts is known as accuracy.

$$Accuracy = \frac{\text{True Positive + True Negative}}{Total\ Samples} \quad (1)$$

Although it provides a general assessment of the model's performance, it could not be accurate when working with datasets that are unbalanced.

C. Precision

Precision quantifies how well optimistic predictions work. When the expense of false positives—such as identifying osteoporosis when the patient does not have it—is substantial, it can be helpful.

$$\text{Precision} = \frac{\text{True Positive}}{\text{True Positive + True Negative}} \quad (2)$$

D. Sensitivity Recall

When the cost of false negatives is significant, recall—a measure of how well the model detects positive samples—becomes critical (e.g., failing to identify someone with osteoporosis).

$$\text{Recall} = \frac{\text{True Positive}}{\text{True Positive + False Negative}} \quad (3)$$

E. The F-1 Score

The F1-score provides a balance between precision and recall by taking the harmonic mean of the two. When you need to take into account both false positives and false negatives, it is really helpful.

$$\mathrm{F}-1\ \mathrm{Score}\ =\ 2\ x\ \frac{\mathrm{Precision\ x\ Recall}}{\mathrm{Precision+Recall}} \quad (4)$$

F. Region Below the AUC-ROC (Receiver Operating Characteristic Curve)

The likelihood that the model will rank a randomly selected positive instance higher than a randomly selected negative instance is represented by the AUC. The True Positive Rate (Recall) is plotted against the False Positive Rate using ROC curves.

AUC is a number between 0 and 1, where 1 represents a perfect model.

G. Loss Function

During training, a loss function measures the model's performance. The Binary Cross-Entropy Loss, sometimes referred to as Log Loss, is frequently employed for classification problems:

$$\mathrm{Loss}=-N1i=1\sum N[yilog(pi)+(1-yi)log(1-pi)] \quad (5)$$

where: The anticipated probability of the positive class is represented by p i, while y i is the actual label (0 or 1).

H. CNNs, or convolutional neural networks

A family of deep learning algorithms called CNNs is made to handle structured grid data, like pictures. In terms of mathematics, CNNs extract features from input images by applying convolution processes. The definition of a convolution operation on an image I with a filter K is:

$$I*K=i,j\sum I(i,j)\cdot K(i,j) \quad (6)$$

Where $**$ indicates the convolution operation and (i,j)(i,j) are pixel coordinates,

$$I*K=\ i,j\sum\ I(i,j)\cdot K(i,j). \quad (7)$$

CNNs usually consist of multiple layers: Convolutional layers: To extract features, apply filters.

Pooling layers: Usually employing max-pooling, these reduce the spatial dimensions of the data.Final predictions are made using fully connected layers, which are based on the features that have been extracted.

IV. Datasheet Description

Source of Data: The data set was fetched from the authentic sources like Kaggle and other medical imaging databases, with good quality and labeling. Such sites provide a set of contributed radiographic images from medical establishments, researchers, and practitioners themselves.

Number of Images: The dataset is composed of [number]X-ray images, which can be broadly categorized into two groups:

A. Non Osteoporotic

Figure 4. Knee X-ray Without Osteoporosis

Figure 4 Illustrates several salient characteristics are noted. First, bone density looks normal, indicating healthy mineralization as the bones show the anticipated whiteness and density on the picture. Second, the joint space between the bones is kept in good condition, indicating that the cartilage that cushions the joint is sufficiently thick and hasn't degraded too much. For movement to be painless and fluid, this proper joint space is essential. Furthermore, there are no indications of thinning, fractures, or anomalies in the bone structure itself, which is smooth and well- defined. In conclusion, a normal knee X- ray shows smooth, well- defined bone structures, good bone density, and proper joint space, which is a sign of healthy cartilage.

B. Osteoporotic

Figure 5. Knee X-ray with Osteoporosis

Figure 5 Illustrates numerous distinguishing characteristics are noted. First of all, compared to a healthy bone, the bones seem less white or more translucent on the imaging due to a decrease in bone density. Osteoporosis is characterized by a loss of bone mineral content, which is reflected in this decreased density. Second, there may be a narrowing of the joint space between the bones. This narrowing indicates a decrease in the thickness of the joint-cushioning cartilage, which may be brought on by co-existing diseases like osteoarthritis or as a side effect of osteoporosis. Pain and reduced movement may result from reduced joint space. Furthermore, there may be indications

of thinning, increased porosity, or even fractures in the actual bone structure, especially near the ends, making it seem less distinct. In conclusion, an X-ray of an osteoporotic knee usually shows reduced bone density, a less defined bone structure with probable thinning or fracture symptoms, and maybe decreased joint spacing suggestive of cartilage loss

V. Preprocessing Steps

Normalizing (pixel values scaled to 0-1), trimming (uniform dimensions, e.g., 224x224, for connection with frameworks like DenseNet, ResNet, and VGG16), augmentation (rotation, tumbling, zooming, contrast adjustment for better the volume of the dataset and generalization), noise elimination (filtering to eliminate documents), and classification (isolating the knee region of interest) were some of the preprocessing steps that were performed on raw image data in order to maximize deep model performance.

VI. Results

The experimental results demonstrate the effectiveness of the proposed deep learning-based method for early osteoporosis detection using X-ray imaging. A standard set of metrics were used to evaluate the model's performance, and the numerical data and visualizations presented here ensure clarity and impact

Table 2 : Performance Categorization

Epoch	Accuracy	Loss	Validation Accuracy	Validation Loss	performance
1	0.4167	1.4362	0.5763	1.1065	Low
2	0.6023	0.9339	0.4806	1.4751	Low
3	0.7260	0.6586	0.5218	1.2568	Moderate
4	0.7669	0.5701	0.5569	1.3000	Moderate
5	0.8771	0.3182	0.5642	1.6816	High
6	0.9382	0.1752	0.6162	1.7986	High

A. Accuracy

It is an expression of the number of correctly classified samples divided by the total number of samples. It reflects an overall performance of the model.

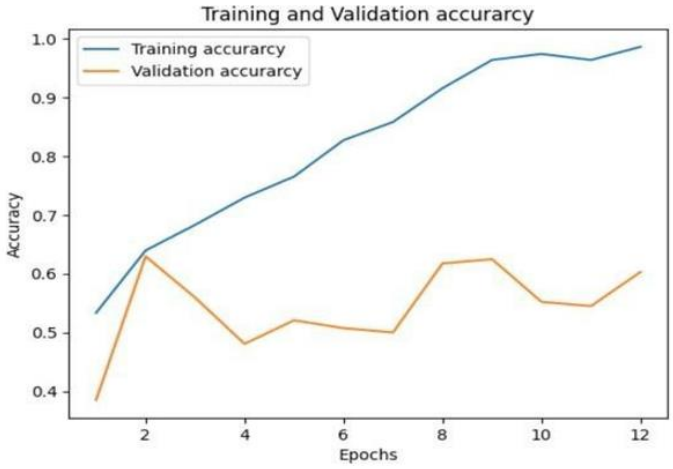

Figure 6. Training and Validation accuracy

Figure 6 Illustrates the model's training and validation accuracy over 12 epochs for osteoporosis diagnosis is depicted in the graph. The training accuracy is represented by the blue line, which gradually rises over the training phase and approaches near-perfect accuracy by the later epochs. This shows that the model is successfully picking up on the patterns in the training set. But the validation accuracy, shown by the orange line, conveys a different message. Although it climbs at first, it plateaus and even fluctuates before performing inconsistently after peaking around the second epoch. The model has become very specialized to the training data and finds it difficult to generalize to unseen data, which is a critical factor for real-world osteoporosis detection. This large discrepancy between training and validation accuracy points to overfitting. This disparity emphasizes

the necessity of methods such as regularization, dropout, or data augmentation to strengthen the model's capacity for generalization and increase its usefulness in osteoporosis screening.

B. Validation Loss

One statistic for assessing a model's performance on data it hasn't seen during training is validation loss. It is computed using the validation set, a distinct subset of the data that isn't utilized for model training, in the same manner as the training loss.

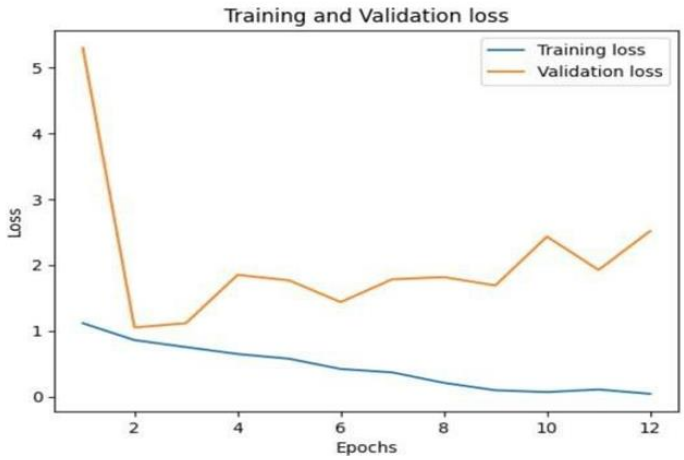

Figure 7 . Training and Validation Loss

Figure 7 Illustrates the training and validation loss of a model designed for osteoporosis diagnosis throughout 12 training epochs is shown in the graph. As training goes on, the model is successfully reducing mistakes on the training data, as shown by the blue line, which represents training loss, which shows a steady downward trend. This implies that the patterns in the training set were successfully learned. A distinct pattern is shown by the orange line, which represents validation loss. After first declining, it starts to fluctuate and eventually rises in subsequent epochs. One of the main signs of overfitting is this difference between training and validation losses. Although the model performs well on the training data, it has trouble generalizing to new data, which is a serious issue for osteoporosis detection in the real world as the model will come across a variety of patient data that was not included in the training set. The model's performance on fresh osteoporosis cases would suffer if it were beginning to memorize the training data instead of learning generalizable features, as indicated by the growing validation loss in later epochs. In order to guarantee strong performance in real-world osteoporosis screening settings, our observation highlights the necessity of overfitting mitigation tactics including regularization techniques, early halting, or training dataset expansion.

C. AUC-ROC Curve

The Area Under the Receiver Operating Characteristic Curve measures the trade-off between sensitivity and specificity. The higher the AUC value, the better the discriminatory capability[13][14]

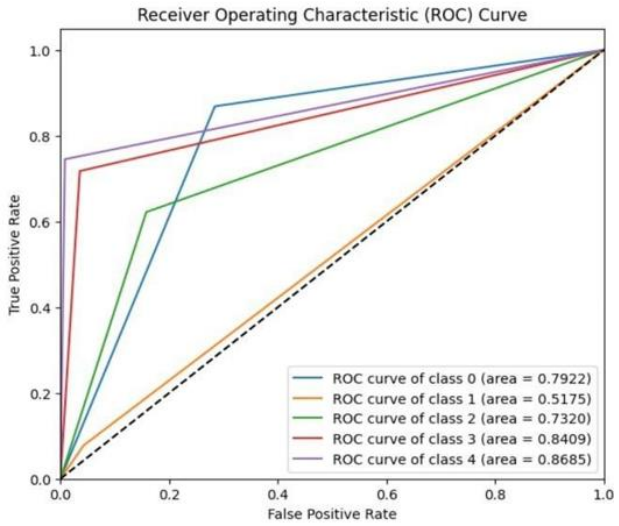

Figure 8: Receiver Operating Characteristic (ROC) Curve

Figure 8 Illustrates the model's ability to detect osteoporosis in five different classes is visually shown by the Receiver Operating Characteristic (ROC) curves in the image. Plotting the True Positive Rate (TPR) versus the False Positive Rate (FPR) for a particular class at different threshold values is what each curve does. A curve with minimal false alarms (FPR) and high sensitivity (TPR) would ideally hug the top-left corner. Better overall performance is shown by a bigger area under each curve (AUC), which is a numerical statistic. A higher AUC in this case would indicate that the model can successfully differentiate between people in the corresponding class who have osteoporosis and those who do not, facilitating early detection and care. Examining each class's ROC curves and AUC values yields useful

D. Confusion Matrix

This visualizes the number of true positives, true negatives, false positives, and false negatives, hence an intuitive understanding of the classification performance of the model

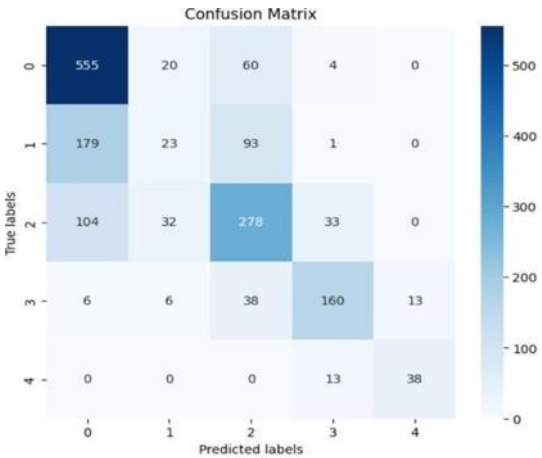

Fig 9. Confusion Matric

Figure 9 Illustrates a thorough analysis of the classification model's performance across five different classes is given by the confusion matrix. Strong prediction accuracy for class 0 (555 instances) and class 2 (278 instances) is revealed by the diagonal elements, which reflect correctly categorized instances. This shows how well the model can detect

these categories. Off-diagonal features, however, draw attention to particular areas of misunderstanding. Significantly, a sizable portion of class 1 examples were incorrectly identified as either class 0 (179 instances) or class 2 (93 instances), indicating possible feature overlap or similarity between these classes. The difficulties in differentiating between these groups were further highlighted by the fact that some class 0 examples were mistakenly assigned to class 2 (60 instances). A fraction was incorrectly classified as class 2 (38 instances), even though class 3 obtained a respectable number of right classifications (160 instances). Overall, Class 4 showed fewer instances—38 were accurately identified. By addressing the observed confusion between particular classes, this examination of the confusion matrix enables a detailed understanding of the model's performance and identifies specific areas for possible improvement.

VII. CONCLUSION

Osteoporosis is a medical condition in which the bones become thin and fragile, and by the time it is noticed, symptoms are usually already severe. Early detection is vital to avoid complications and improve patient outcomes. In this study, a model for detecting osteoporosis using knee X-rays with advanced Convolutional Neural Network architectures such as Xception is proposed, taking advantage of popular machine learning frameworks such as Tensor Flow and Keras. These tools enable the model to extract and classify features efficiently from X-ray images with high accuracy and reliability. The model development process consisted of several critical stages including data preprocessing, feature extraction, and model training. Libraries such as NumPy were used for efficient data manipulation. Matplotlib provided visualization support to analyze the transformations done on images and the model's performance. Scikit-learn was used to calculate the accuracy, precision, and recall of the model by using robust metrics and classification techniques .Other utility libraries streamlined the workflow, so the implementation was efficient and scalable. In conclusion, this study shows potential machine learning applications in the diagnosis of diseases, focusing on early disease detection through the application of AI in healthcare systems. Such solutions may significantly alter osteoporosis management, with timely interventions being better for patients.

Reference

[1] Manjunatha, M.B. (2018). Design and Development of ASL Recognition by Kinect Using Bag of Features. In: Reddy, M., Viswanath, K., K.M., S. (eds) International Proceedings on Advances in Soft Computing, Intelligent Systems and Applications. Advances in Intelligent Systems and Computing, vol 628. Springer, Singapore. https://doi.org/10.1007/978-981-10-5272-9_31

[2] Pramod K.B. Rangaiah, and Robin Augustine Improving burn diagnosis in medical image retrieval from grafting burn samples using B-coefficients and the CLAHE algorithm, Biomedical Signal Processing and Control, Volume 99, 2025, 106814, ISSN 1746-8094, https://doi.org/10.1016/j.bspc.2024.106814

[3] Darshan, S.L.S., Naresh, E. et al. Design of Chest Visual Based Image Reclamation Method Using Dual Tree Complex Wavelet Transform and Edge Preservation Smoothing Algorithm. SN COMPUT. SCI. 5, 352 (2024). https://doi.org/10.1007/s42979-024-02742-3

[4] Srinidhi, N.N., Shiva Darshan, S.L. et al. Design of Cost Efficient VBIR Technique Using ICA and IVCA. SN COMPUT. SCI. 5, 560 (2024). https://doi.org/10.1007/s42979-024-02936-9

[5] Swaminathan, S. V., Surendiran, J., (2019). Design and Implementation of Kogge Stone adder using CMOS and GDI Design: VLSI Based. International Journal of Engineering and Advanced Technology (IJEAT), 8(6S3).\

[6] Robin Augustine,"Enhancing Medical Image Reclamation for Chest Samples Using B-Coefficients, DT-CWT and EPS Algorithm," in IEEE Access, vol. 11, pp. 113360-113375, 2023, doi: 10.1109/ACCESS.2023.3322205

[7] Manjunatha, M. B. (2017). A hybrid gesture recognition method for American sign language. Indian Journal of Science and Technology, 10(1), 1-12.

[8] Manjunatha, M. (2016). Performance analysis of KNN, SVM and ANN techniques for gesture recognition

system. Indian Journal of Science and Technology, 9(1), 1-8.

[9] Prathap, C., & Dharshith, C. (2013). An automatic approach for segmentation of ultrasound liver images. Journal of Emerging Technology and Advanced Engineering, 3(1), 20-2.

[10] Naresh, E., Ashwitha, A., Reddy, K. T., & Srinidhi, N. N. (2025). The Burn Grafting Image Reclamation Redefined with the Peak-Valley Approach. Critical Reviews™ in Biomedical Engineering, 53(2).

[11] Ravikumar, J. Gauging Deep Learning Archetypal Effectiveness in Haematological Reclamation. SN COMPUT. SCI. 5, 963 (2024). https://doi.org/10.1007/s42979-024-03322-1

[12] Rangaiah PKB, Histopathology-driven prostate cancer identification: A VBIR approach with CLAHE and GLCM insights. Comput Biol Med. 2024 Oct 1;182:109213. doi: 10.1016/j.compbiomed.2024.109213. Epub ahead of print. PMID: 39357133.

[13] Fredrik Huss et al. Precision Diagnosis of Burn Injuries: Clinical Implications of Imaging and Predictive Modeling, 09 October 2024, PREPRINT (Version 1) available at Research Square [https://doi.org/10.21203/rs.3.rs-5002889/v1]

[14] Manoj, H.M. Comparative Assessment of Machine Learning Models for Predicting Glucose Intolerance Risk. SN COMPUT. SCI. 5, 894 (2024). https://doi.org/10.1007/s42979-024-03259-5

[15] Augustine, Robin, Improving Liver Cancer Diagnosis: A Multifaceted Approach to Automated Liver Tumor Identification in Ultrasound Scans. Available at SSRN: https://ssrn.com/abstract=4646452 or http://dx.doi.org/10.2139/ssrn.4646452

[16] Pramod K.B. Rangaiah, and Robin Augustine Improving burn diagnosis in medical image retrieval from grafting burn samples using B-coefficients and the CLAHE algorithm, Biomedical Signal Processing and Control, Volume 99, 2025, 106814, ISSN 1746-8094, https://doi.org/10.1016/j.bspc.2024.106814.

[17] Augustine, Robin, Vbir-Based Assessment of Radiographic-Divergence Agent Attention in Prostate Melanoma Patients. Available at SSRN: https://ssrn.com/abstract=4752359 or http://dx.doi.org/10.2139/ssrn.4752359

[18] Rangaiah, Pramod and Augustine, Robin, Enhanced Glaucoma Detection Using U-Net and U-Net+ Architectures Using Deep Learning Techniques. Available at SSRN: https://ssrn.com/abstract=4831407 or http://dx.doi.org/10.2139/ssrn.4831407

[19] L. R, S. A R, M. M. Ibrahim and S. V, "Hybrid Threshold Speech Enhancement Scheme Using TEO And Wavelet Coefficients," 2023 Second International Conference on Electrical, Electronics, Information and Communication Technologies (ICEEICT), Trichirappalli, India, 2023, pp. 01-05, doi: 10.1109/ICEEICT56924.2023.10156921

[20] Prasad, S., Samimalai, A., Rani, S.R., Kumar, Hegde, N., Banu, S. (2023). Information Security and Privacy in Smart Cities, Smart Agriculture, Industry 4.0, Smart Medicine, and Smart Healthcare. In: Joby, P.P., Balas, V.E., Palanisamy, R. (eds) IoT Based Control Networks and Intelligent Systems. Lecture Notes in Networks and Systems, vol 528. Springer, Singapore.

[21] Pramod K B, Kumaraswamy H.V, Prathap C and M. Swamy, "Design and analysis of UHF BJT feedback oscillator using linear and non-linear simulation," 2013 International Conference on Emerging Trends in Communication, Control, Signal Processing and Computing Applications (C2SPCA), Bangalore, India, 2013, pp. 1-6, doi: 10.1109/C2SPCA.2013.6749386.

[22] V. C, S. A. R, B. D and S. V, "Speech-to-text Transfiguration in Language Numerals for Perpetual Deaf Patients," 2023 Second International Conference on Electrical, Electronics, Information and Communication Technologies (ICEEICT), Trichirappalli, India, 2023, pp. 1-5, doi: 10.1109/ICEEICT56924.2023.10157113.

[23] Surendiran, R. Reenadevi, R. G. Vidhya, S. S. Sivasankari, and N. Balaji, "IoT-Based Advanced Electric Vehicle Charging Infrastructure," 2022 Fourth International Conference on Cognitive Computing and Information Processing (CCIP), Bengaluru, India, 2022, pp. 1-6, doi: 10.1109/CCIP57447.2022.10058649.

[24] Manoj, H. M., Anil, C., & Rohith, S. (2021, June). An Novel Hand Gesture System for ASL using Kinet

Sensor based Images. In Proceedings of the First International Conference on Computing, Communication and Control System, I3CAC 2021, 7-8 June 2021, Bharath University, Chennai, India

[25] Kumar, B. P. (2019). Framework of ASL Silhouette Gesture Recognition System. In Blue Eyes Intelligence Engineering & Sciences Publication (Vol. 8, No. 6s, pp. 66-72).

[26] P. P. Kumar et al., "Advanced Electric Vehicle Charging Infrastructure Using Internet of Things," 2022 3rd International Conference on Communication, Computing and Industry 4.0 (C2I4), Bangalore, India, 2022, pp. 1-6, doi: 10.1109/C2I456876.2022.10051342.

[27] Naresh, S. V. N. Murthy, P. K. Pareek, K. T. Reddy, S. L. Shiva Darshan and B. P. P. Kumar, "DevOps Life Cycle Implementation on Real Life Scenarios," 2024 International Conference on Knowledge Engineering and Communication Systems (ICKECS), Chikkaballapur, India, 2024, pp. 1269-1271, doi: 10.1109/ICKECS61492.2024.10617200

[28] Kumar C., A. ., G. R., P. ., G. R., P. ., R., A. ., B. P., P. K. ., S., H. ., & Vaishnavi D. A., L. . (2024). Implementation of an Efficient and Reconfigurable Architecture for DCT on FPGA. International Journal of Intelligent Systems and Applications in Engineering, 12(10s), 597–604.

[29] Mallanna, S. D. “High Gain Perfect Matched Inset Fed Rectangular Microstrip Patch Antenna for 2.4 GHz Frequency” Journal of Adv Research in Dynamical & Control Systems, , Vol. 10, 13-Special Issue, 2018

[30] Surendiran, S.Subburam, F. S. K, S. SS, G. Saritha "An Extensive Analysis of Amphibious Drones for Surveillance," 2024 International Conference on Power, Energy, Control and Transmission Systems (ICPECTS), Chennai, India, 2024, pp. 1-6, doi: 10.1109/ICPECTS62210.2024.10780083.

[31] S.Subburam, F. S. K, S. SS, G. Saritha and J.Surendiran, "Gesture Recognition using IR sensor camera," 2024 International Conference on Power, Energy, Control and Transmission Systems (ICPECTS), Chennai, India, 2024, pp. 1-6, doi: 10.1109/ICPECTS62210.2024.10780010.